Photodissociation of Triatomic Hydrogen

P. C. Cosby and H. Helm
Molecular Physics Department, SRI International, Menlo Park, California 94025
(Received 2 May 1988)

We report the first observation of photodissociation of H_3. Predissociation of the optically prepared $3s\,^2A_1'$ and $3d\,^2E''$ states by the $\tilde{X}\,^2E'$ ground state is detected by monitoring of the production of rovibrationally excited H_2 molecules and H atoms. Product excitation is found to be highly dependent on H_3 electronic and nuclear configuration.

PACS numbers: 33.80.Gj, 34.50.Lf, 34.50.Pi

The unstable ground-state potential surface of H_3 has served as prototype for the development of bimolecular reaction-rate theory,[1] and is still largely territory only of theoretical chemistry. While the ground electronic state of H_3 is dissociative, electronically excited states of this molecule are tightly bound.[2-4] These states are described in terms of a Rydberg electron bound by the field of the stable, triangular H_3^+ core. Since the first experimental indication[5] of a stable H_2 molecule was obtained in 1968, rapid progress has been made in the characterization of its bound excited states.[6-11]

We report here a study of photodissociation of the H_3 molecule with high-resolution kinetic-energy analysis of the H_2+H fragments. Using optical excitation of predissociated states of H_3, we gain selective access to the unstable ground-state surface, under conditions where all relevant quantum numbers of the system, the total energy, and the geometry of the transition state are defined within the uncertainty principle limit. The half-collision of the selected transition state is mapped out by measurement of the translational and internal energy content of the $H_2(v,J)+H$ fragments.

The experiments were performed in the SRI fast-neutral-beam photofragment spectrometer, which has been described recently.[12] H_3 molecules are formed by near-resonant charge transfer[13] of H_3^+ in a Cs vapor cell. Approximately 1.4 μs after formation the H_3 beam intersects at right angles the intracavity beam of a cw dye laser. Photodissociation fragments are detected on a position-sensitive detector for correlated particles. This detector explicitly measures the distance between the fragments (R) and their temporal separation (Δt). From these quantities[14] the center-of-mass energy release W with which the molecule ejected two fragments with masses M and m is determined for each fragment pair H_2+H. The separation of the fragments R is the sum of the individually measured radial distances of each fragment from the center of the detector: $R=R_m+R_M$. The ratio R_m/R_M for the photodissociations reported here was peaked at 2, as expected for the reaction:

$$H_3+h\nu\rightarrow H+H_2.$$

Approximately 10% of the observed photofragments yielded ratios in a broad distribution centered at unity. These fragments reflect photodissociation of H_3 into three H atoms (two of which are observed by the detector), but we will not consider this process further here.

In the absence of the laser, a small fraction of the neutral beam is observed to fragment by spontaneous decay within the 8.7-cm interval between the beam defining slit and the beam terminating flag (see Fig. 3 of Ref. 12). When the laser is turned on, no variation in this dissociation rate is observed except at six discrete wavelengths in the range of 577–603 nm. A plot of the observed fragment flux (for fragments produced with $W\geq 4$ eV) as the laser is tuned over this wavelength range is shown in Fig. 1. The two strong transitions labeled $3dv_0$ and $3sv_0$ in this figure occur at the wavelengths reported by Herzberg and co-workers[6-10] for transitions between the long-lived,[13] vibrationless H_3 $2_p^2A_2''(N=K=0)$ level and the $(N=1)$ levels of the H_3 $3d\,^2E''$ and $3s\,^2A_1'$ states, respectively.

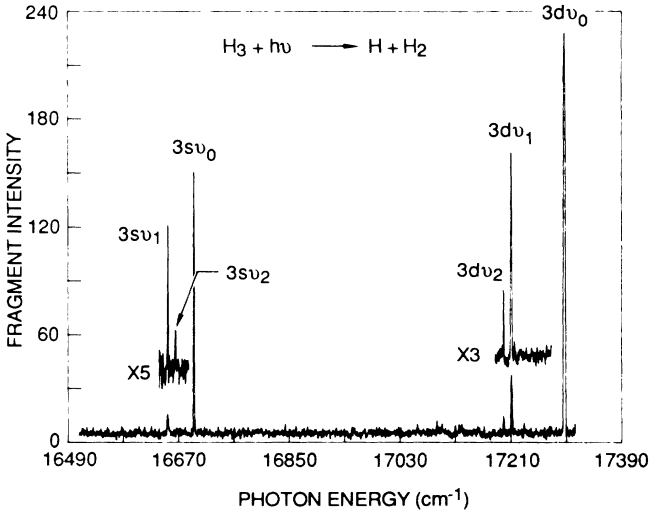

FIG. 1. Observed production of photofragments from H_3 as a function of the photon energy of the exciting laser. Only photofragments produced with $W\geq 4$ eV are recorded for this spectrum. The spectrum at other energy releases is similar, but with a substantial background due to spontaneous dissociation fragments.

TABLE I. Observed photodissociation transitions in H_3.

Label	Observed line[a] (cm^{-1})	Identification Upper state (v_1', v_2', N', K')	Identification Lower state (v_1'', v_2'', N'', K'')	Reported line[b] (cm^{-1})	Measured upper state energy[c] (eV)
$3dv_0$	17297.6	$3d\,^2E''(0,0,1,1)$	$2p\,^2A_2''(0,0,0,0)$	17296.982	7.706 ± 0.028
$3dv_1$	17211.6	$3d\,^2E''(1,0,1,1)$	$2p\,^2A_2''(1,0,0,0)$		8.115 ± 0.024
$3dv_2$	17199.1	$3d\,^2E''(0,1,1,1)$	$2p\,^2A_2''(0,1,0,0)$		8.011 ± 0.028
$3sv_0$	16695.6	$3s\,^2A_1'(0,0,1,0)$	$2pA_2''(0,0,0,0)$	16694.972	7.634 ± 0.020
$3sv_2$	16665.7	$3s\,^2A_1'(0,1,1,0)$	$2p\,^2A_2''(0,1,0,0)$		
$3sv_1$	16653.6	$3s\,^2A_1'(1,0,1,0)$	$2p\,^2A_2''(1,0,0,0)$		8.042 ± 0.028

[a]Estimated accuracy ± 1.5 cm^{-1}.
[b]References 7 and 10.
[c]Relative to $H(1s)+H_2\,X\,^1\Sigma_g^+(v=0, J=0)$.

The remaining four lines that appear in Fig. 1 are identified as transitions from the $2p\,^2A_2''(N=K=0)$ level with one quantum of vibration in the symmetric stretch v_1 and bending v_2 vibrational modes into the corresponding levels of the $3d$ and $3s$ states. The measured transition energies and identifications of all six lines are given in Table I. These assignments are based on the energy and angular distributions measured for their photofragments.

The production of photofragments can be understood from the radiative and dissociative pathways that exist for the H_3 molecule (see Fig. 2). The energies of the relevant H_3 states have been established in the work of Herzberg and co-workers,[6-10] Watson,[15] and Vogler.[16] Transitions observed in the present work are denoted by the solid vertical arrows, and radiative transitions connecting the states are denoted by the dashed arrows. The six possible dissociation channels, denoted by horizontal arrows and labeled I–VI, are indicated, together with their expected fragment energies (W) for dissociation to the lowest-energy products $H(1s)+H_2\,X(v=0, J=0)$.

The center-of-mass kinetic-energy releases (W) observed from the dissociation of H_3 into $H+H_2$ products

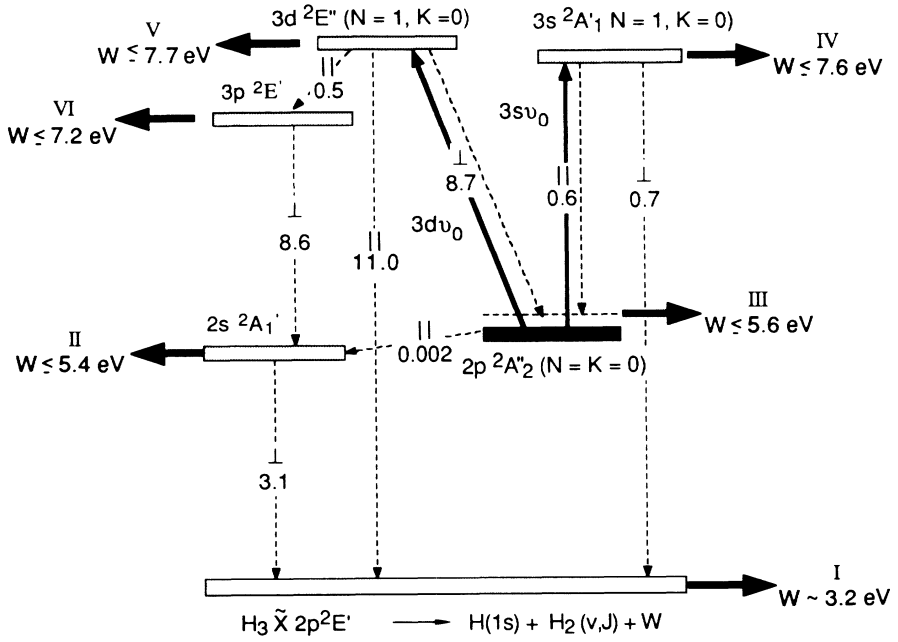

FIG. 2. Radiative connections among the H_3 electronic states access from the $2p\,^2A_2''(N=K=0)$ metastable level. Photoabsorption transitions are shown by the two solid vertical arrows, spontaneous emission by the dashed arrows. Theoretical transition rates (in units of 10^7 s^{-1}) and the orientation of the transition moment relative to the C_3 axis of H_3 are given for each. Predissociation channels are labeled by I–VI, with expected maximum fragment energy releases given for each.

are shown in Fig. 3. The two upper spectra refer to photodissociation via the $3s$ and $3d$ states of the vibrationless molecule. The lower part is the energy-release spectrum observed in the absence of photons, or with the laser not tuned to one of the six transitions. A major contribution to this spontaneous dissociation arises from the very slow ($\tau \sim 50$ μs) radiative decay of the $2p^2A_2''(N=K=0)$ molecules into the $2s^2A_1'(N=1,K=0)$ level. The latter is rapidly predissociated,[7,10] producing fragments in channel II (Fig. 2).

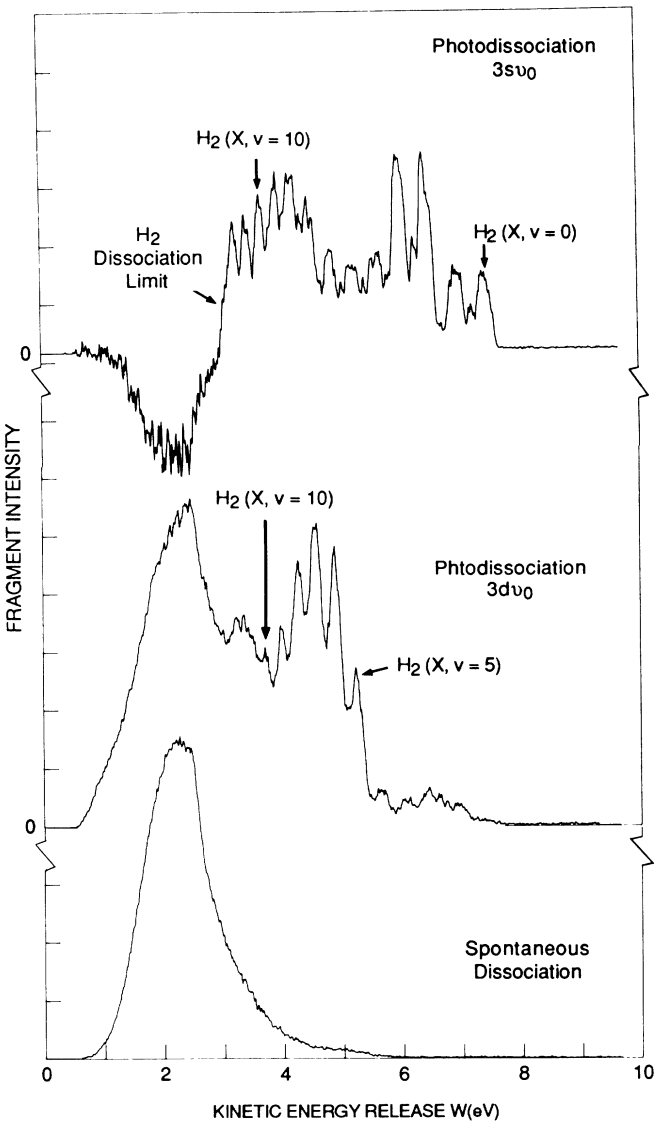

FIG. 3. Fragment kinetic-energy releases (W) accompanying the production of $H+H_2$ from H_3. Fragmentation observed as a result of spontaneous dissociation is shown in the lower portion of the figure, while that observed to accompany absorption in the $3dv_0$ and $3sv_0$ transitions is shown in the center and upper portions of the spectrum, respectively. Selected vibrational levels of the H_2 $X^1\Sigma_g^+$ photofragments are identified in the figure. All spectra have been corrected for the collection efficiency of the apparatus.

The photodissociation-fragment energy spectra in the center and top portions of Fig. 3 show considerable structure. For both spectra, the laser was chopped and fragments observed with the laser off were subtracted from those observed with the laser irradiating the beam. In the $3sv_0$ spectrum (top), the structure is clearly assignable to the production of H_2 photofragments in vibrational levels $v=0$–10 via channel IV. The anharmonicity of the H_2 molecule makes the assignment completely unique. Moreover, subsidiary rotational structure is resolved in a number of the vibrational levels, most notably $J=7$ in $v=0$, 2, 4, 5, and 7. Preliminary modeling of the rotational contributions within each vibrational peak suggests a highly nonequilibrium distribution peaking at $J=5$ in the lower vibrational levels. Only two peaks appear in the spectrum with energy releases below that corresponding to H_2 ($v=10$), whereas there are fifteen bound vibrational levels[17] in the nonrotating molecule. We tentatively assign these two peaks to H_2 ($v=11, J=7$) and ($v=12, J=9$), suggesting a higher propensity for strong rotational excitation when the H_2 photofragment is produced near its dissociation limit. This is consistent with the lack of photofragments corresponding to $v=13$ and 14, since both these vibrational levels are unbound for this degree of rotational excitation.

Structure also appears in the kinetic-energy spectrum of $H+H_2$ produced when the $3d^2E''(N=1,K=0)$ level is excited, as shown in the center of Fig. 3. This structure is uniquely identified as predissociation of the $3d$ state via channel V (Fig. 2). The H_2 fragments are produced with a distribution of vibrational levels quite different from those observed when $3sv_0$ is pumped. The H_2 fragments produced in a given v,J level are found to have higher translational energies by 0.072 ± 0.010 eV when those produced from predissociation of the $3s^2A_1'$ level. This is consistent with the $3d^2E''(N=1,K=1)$-$3s^2A_1'(N=1,K=0)$ energy separation of 0.07464 eV established by Herzberg and co-workers.[6-10]

At lower kinetic-energy releases ($W \leq 3$ eV), below the kinematic limit for dissociation into $H+H_2$ via channels IV and V, the spectra from $3s^2A_1'$ and $3d^2E''$ excitation are also dramatically different. When the $3s^2A_1'$ state is excited, fewer fragments are produced in this energy range when the laser is tuned to the $3sv_0$ transition than when it is turned off. Since the $2p^2A_2''(N=K=0)$ level is the ultimate parent in both the spontaneous-dissociation process II and the photofragment process IV, depletion of population in this level by photodissociation will produce a corresponding decrease in the number of spontaneous dissociations occurring while the laser is irradiating the H_3 beam. From Fig. 2, it is clear that in order for such a depletion to be observed, the rate for radiative decay of the $3s^2A_1'$ state must be slower than its direct predissociation.

In contrast, photoexcitation of the ground vibrational

level of the $3d^2E''$ state, shown in the center of Fig. 3, gives rise to an *increase* in the low-energy photofragments. This suggests that the rate for radiative decay of $3d^2E''$ into the ground state or into $2p^2A_2''(N=2,K=0)$ is comparable with its rate of predissociation.

The measured fragment energies establish the energies of the photoexcited H_3 levels absolutely with respect to the $H(1s)+H_2$ $X^1\Sigma_g^+(v=0,J=0)$ dissociation limit. These energies are given in the last column of Table I. The energy of the absorbing $2p^2A_2''(N=K=0)$ level relative to this same limit is obtained from these values by subtraction of the photon energy that produced the transition. This places the ground vibrational level of the H_3 $2p^2A_2''(N=K=0)$ state 5.563 ± 0.020 eV above this dissociation limit.

The $3s^2A_1'$ and $3d^2E''$ levels which are observed to predissociate here are, at least superficially, quite similar. Each state has a total angular momentum $J=1$ and is described by an *ortho* H_3^+ core tumbling end over end as characterized by the quantum numbers $N^+=1$, $K^+=0$. Both states predissociate by vibronic coupling and access the ground-state surface at nearly the same energy: The $3s^2A_2''$ at an energy 7.634 eV above the $H+H_2$ dissociation limit and the $3d^2E''$ at an energy only 0.074 eV higher. Nevertheless, the two states produce dramatically different dissociation product distributions, suggesting that the evolution into continuum states is greatly influenced and by the instantaneous distribution of momenta in this six-particle system and the topography of the ground state. We anticipate that quantitative rovibrational populations for the H_2 fragment can be derived from the photofragment data to provide a detailed probe into the dynamical properties[18] of the ground-state potential surface of H_3.

We gratefully acknowledge many helpful discussions during the course of this work with Dr. David L. Huestis, Dr. Roberta P. Saxon, and numerous other coworkers at SRI International. This research was supported by U.S. Air Force Office of Scientific Research Contract No. F49620-87-K-0002.

[1]H. Eyring, H. Gershinowitz, and C. E. Sun, J. Chem. Phys. **3**, 786 (1935).

[2]H. F. King and K. Morokuma, J. Chem. Phys. **71**, 3213 (1979).

[3]M. Jungen, J. Chem. Phys. **71**, 3540 (1979).

[4]R. L. Martin, J. Chem. Phys. **71**, 3541 (1979).

[5]F.-M. Devienne, C. R. Acad. Sci. Paris B **267**, 1279 (1968).

[6]G. Herzberg, J. Chem. Phys. **70**, 4806 (1979).

[7]I. Dabrowski and G. Herzberg, Can. J. Phys. **58**, 1238 (1980).

[8]G. Herzberg and J. K. G. Watson, Can. J. Phys. **58**, 1250 (1980).

[9]G. Herzberg, H. Lew, J. J. Sloan, and J. K. G. Watson, Can. J. Phys. **59**, 428 (1981).

[10]G. Herzberg, J. T. Hougen, and J. K. G. Watson, Can. J. Phys. **60**, 1261 (1982).

[11]H. Helm, Phys. Rev. Lett. **56**, 42 (1986).

[12]H. Helm and P. C. Cosby, J. Chem. Phys. **86**, 6813 (1987).

[13]G. I. Gellene and R. F. Porter, J. Chem. Phys. **79**, 5975 (1983).

[14]D. P. deBruijn and J. Los, Rev. Sci. Instrum. **53**, 1020 (1982).

[15]J. K. G. Watson, Phys. Rev. A **22**, 2279 (1980).

[16]M. Vogler, Phys. Rev. A **19**, 1 (1979).

[17]P. R. Bunker, C. J. McLarnon, and R. E. Moss, Mol. Phys. **33**, 425 (1977).

[18]K. C. Kulander and J. C. Light, J. Chem. Phys. **85**, 1938 (1986).